

Large-Signal Nonlinear Model of a Highly Integrated Quad-Band GSM Transmit Front-End Module

Y. Tkachenko, S. Boerman, H-C. Chung, P. DiCarlo, M. Gerard, J. Gering, J. Hu, A. Klimashov, K. Kwok, P. Reginnella, S. Sprinkle, C. Wei and Y. Yang

Skyworks Solutions, 20 Sylvan Road, Woburn, MA 01801, Gene.Tkachenko@skyworksinc.com

Abstract

A large-signal nonlinear model was developed for a highly integrated quad-band (UGSM/EGSM/DCS/PCS) transmit front-end module (TX-FEM). The model includes separately validated large-signal nonlinear models of HBT amplifiers; large-signal nonlinear PHEMT switch models; large-signal nonlinear Si BJT PA controller model; large-signal EM-co-simulated model of a dual-band directional coupler-detector, including large-signal GaAs MESFET diodes; and Momentum or lumped element based model of the multi-chip module (MCM) level passive networks. To authors' best knowledge this is the highest complexity large-signal transistor-based model of a radio sub-system ever reported.

INTRODUCTION

Higher levels of PA and transmit module complexity [1-3] and aggressive design cycles for new products are driving the need for more accurate models of these RF systems, including models of all active and passive components placed into a module and their interactions. Robust nonlinear models are required that are capable of predicting large-signal module parameters critical for meeting the product specifications, such as output power, efficiency, nonlinearity, etc. Such models provide valuable insight into MCM operation and serve as powerful tools in their design and optimization.

In this paper we present a model of a quad-band (UGSM/EGSM/DCS/PCS) TX-FEM, which integrates two power amplifiers, a PA controller (PAC), T/R switches with controller, a dual-band directional detector/coupler, a diplexer, matching networks and harmonic filters in a single, 50 Ω input and output, 9x10x1.5mm package [3]. The module schematic is shown in Figure 1. It employs InGaP/GaAs HBT, AlGaAs/InGaAs/AlGaAs PHEMT, GaAs epi MESFET Schottky/passive, and Si Schottky/bipolar/CMOS semiconductor technologies. The module delivers 34dBm Pout with 45% PAE at UGSM/EGSM and 31dBm Pout and 36% PAE at DCS/PCS, while meeting a VSWR>20:1 open loop ruggedness spec.

HBT PA models

The three-stage InGaP/GaAs HBT PA IC models are developed using scalable large area HBT array models of up to 11,000 μm^2 in area developed in-house. These array models are based on the VBIC core unit cell model with extrinsic passive elements describing parasitic elements

associated with combiner networks for multiple cells [4], as shown in Figure 2a. Extrinsic element values are extracted for individual array sizes and then fitted for different array sizes using table-based approach and resulting in a single model for a variety of cells.

The model is validated for different unit cell types and different array sizes using IV, over temperature, s-parameter, power, PAE, load-pull and non-linearity (inter-modulation distortion and ACPR) characteristics. Figures 2b-e demonstrate some of the simulated characteristics using the HBT array model, which are in good agreement with the measured data: Figure 2b compares the measured vs. modeled output IV characteristics of the 960 μm^2 HBT array under forced Ib operation; Figure 2c shows measured and modeled bias-dependent S-parameters of the 960 μm^2 HBT array; Figure 2d demonstrates good agreement between the measured and modeled power, gain, PAE and Ic characteristics of a 3600 μm^2 HBT array under a particular bias, drive, input and output loading conditions during on-wafer power sweep; Figure 2e shows the model prediction of the 3rd and 5th order inter-modulation distortion products under a load-pull sweep across the whole Smith chart being in good agreement with measurements.

The models of PA IC's with the Si PA controller were validated separately in a generic quad-band module environment without any post-PA components, except the output matching networks. Si BJT models of the PAC were based on the models provided by the foundry. Figure 3 shows reasonable agreement between the measured and modeled PA module Gain, Pout and PAE characteristics vs. the swept Si controller input voltage.

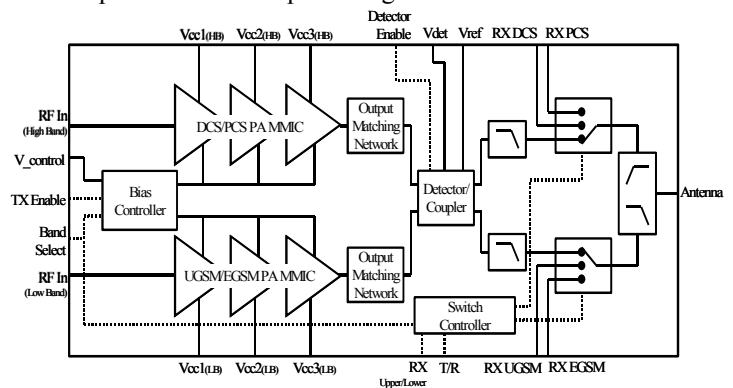


Figure 1. TX-FEM block diagram.

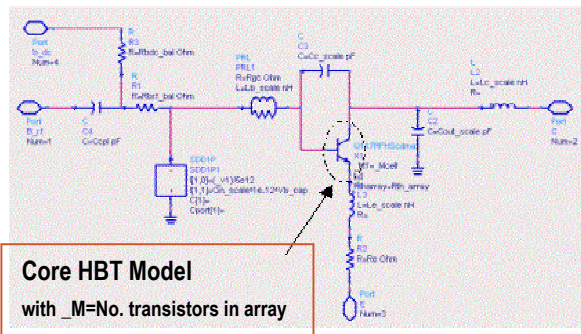


Figure 2a. HBT array model diagram.

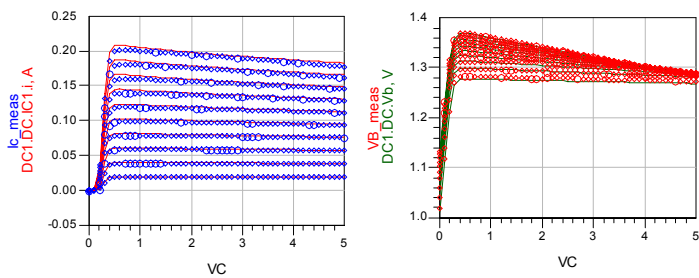


Figure 2b. Modeled vs measured IV characteristics of a $960\mu m^2$ HBT array under forced I_b conditions.

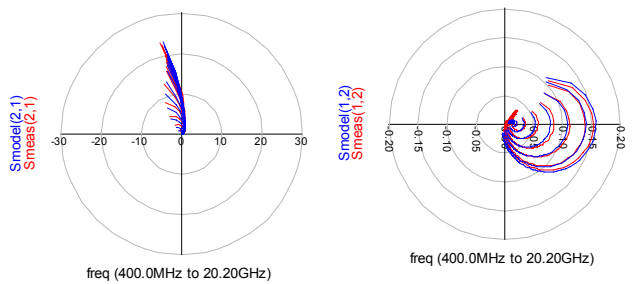
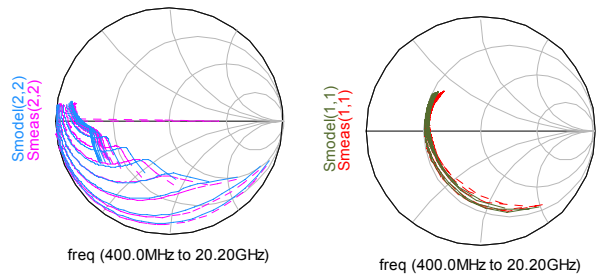


Figure 2c. Measured S-parameters of a $960\mu m^2$ array vs. large-signal HBT array model. $V_{cb}=0.5V$, $I_b=8e-6$ to $1.6mA$.

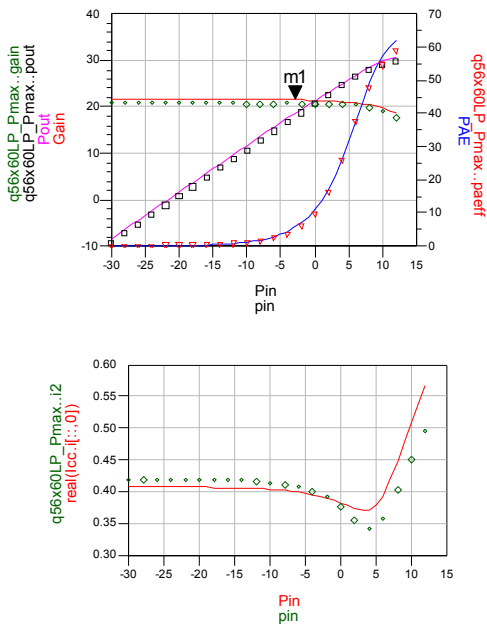


Figure 2d. Measured (symbols) vs. modeled (lines) Gain, P_{out} , PAE and I_c characteristics of a $3600\mu m^2$ HBT array under on-wafer power sweep test. 900 MHz , $V_c=3.2V$, $I_{c0}=420mA$. $\Gamma_{Load}=0.81<177.7$, $\Gamma_{Source}=0.68<164.7$

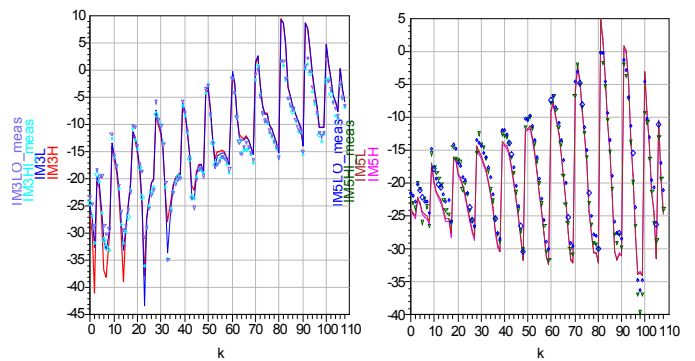


Figure 2e. Measured (symbols) vs. modeled (lines) two-tone inter-modulation distortion characteristics (IM_3 and IM_5 in dBm) of the $960\mu m^2$ HBT array during loadpull test at 900 MHz , $3.2V$, $P_{in}=-2dBm$. Index k specifies a particular load state, with the entire state space covering roughly a $VSWR=7:1$ circle on the Smith chart.

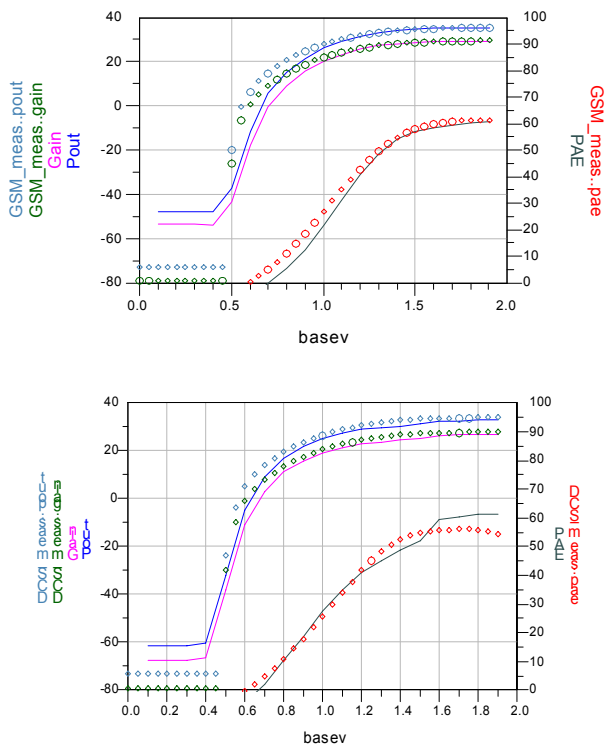


Figure 3. Measured (symbol) vs. modeled (line) GSM and DCS characteristics of a generic quad-band PA module. 900 and 1750 MHz, $V_{cc}=3.2V$, $P_{in}=6dBm$.

PHEMT SP3T models

SP3T switch models are based on the previously reported in-house developed single-gate and multi-gate large-signal nonlinear PHEMT models [5-6]. These models take into account charge conservation, dispersion and self-heating and incorporate accurate models of leakage currents. As shown in Figure 4, the critical capacitance nonlinearities in the device are well predicted by the model. Figure 5 demonstrates good prediction of the insertion loss and isolation by the model. The 2nd and 3rd harmonic behavior vs. control voltage and power is also predicted well.

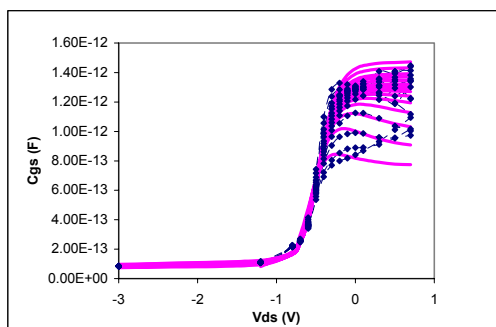


Figure 4. Measured vs. modeled PHEMT C_{gs} characteristics.

Coupler-Detector Model

Large-signal model of the dual-band 900/1800 MHz directional coupler-detector was constructed based on the

large-signal GaAs epi-based Schottky diode models for the reference and detector diodes and Momentum-based EM model of the directional couplers, which were also built on the GaAs die (Figure 6). Measurement-based s-parameter model library was constructed for the MCM level resistor, inductor and capacitor components. Models for the external biasing and matching components of the coupler-detector were taken from this library. Figure 7 shows detected voltage vs. input power simulations based on the models of the two different coupler-detector designs, which were in agreement with the measurements. While the detected voltage characteristics for these two designs are relatively similar, as shown in Figure 8, the difference in the 5th GSM harmonic distortion between them can be as much as 20dB. This result was in agreement with the overall 5th harmonic level of the entire TX-FEM and helped pinpoint the source of distortion being the coupler-detector, not PA or a switch, and select the best design for the overall module performance.

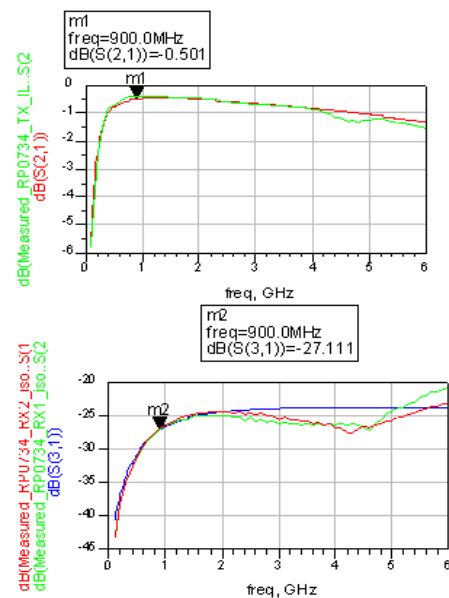


Figure 5. Measured vs. modeled insertion loss and isolation characteristics of an SP3T PHEMT switch.

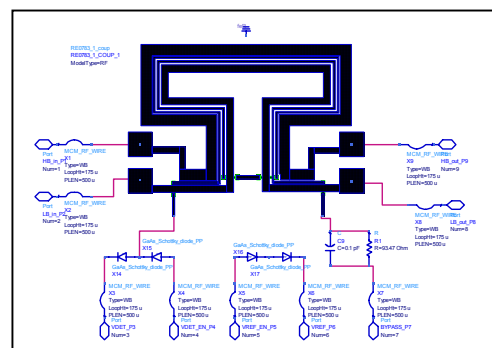


Figure 6. Large-signal GaAs coupler-detector model using Momentum EM co-simulated coupler model and large-signal diode models. Library-based bias and match components are added externally.

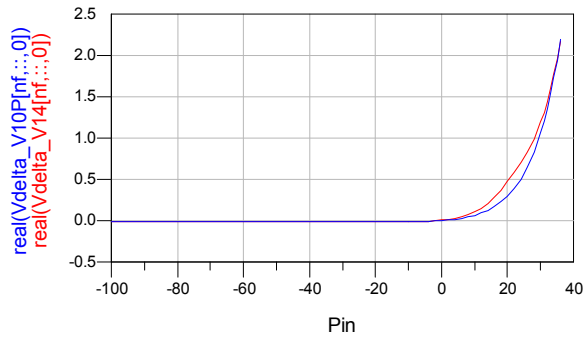


Figure 7. Detected voltage vs. input power simulated for two different coupler-detector designs using large-signal models.

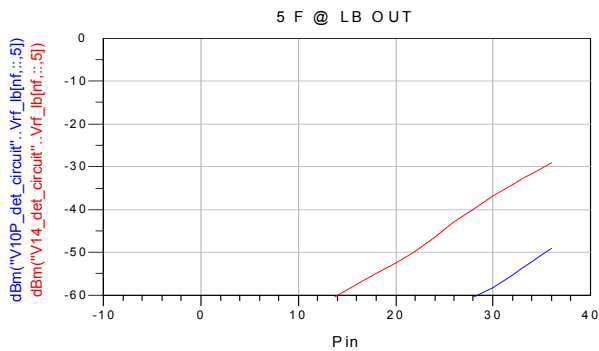


Figure 8. 5th GSM harmonic level simulated using the large-signal models for two different coupler-detector designs.

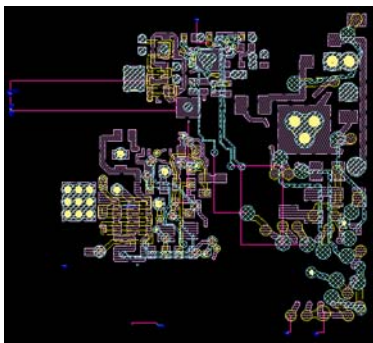


Figure 9. Schematic of a 60-port s-parameter block representation of the post-PA output passive network on the MCM, EM simulated in Momentum.

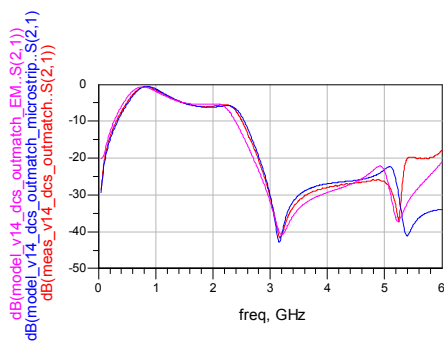


Figure 10. Measured vs. modeled (EM and lumped element) s-parameters of the post-PA IC output passive network.

MCM level passive network modeling

Passive elements including dc and rf lines located at various MCM levels, inter-level and grounding vias were simulated in Momentum and represented as a 60-port s-parameter block for large-signal module simulations. Figure 9 shows the diagram of this highly complex geometrical shape. Passive SMT element models for capacitors, filters and diplexer were connected externally to the s-parameter block ports. Figure 10 compares simulated EM and lumped element model s-parameters to measured data, which was obtained by probing directly on the module.

CONCLUSIONS

Components of a highly integrated quad-band transmit front-end module large-signal model are described. Robust core HBT, PHEMT, Si BJT, FET diode cell and array models, combined with EM co-simulated or measurement-based passive IC level and module level passive components, form a complete large-signal transistor level module simulation environment. This high complexity TX-FEM model constructed provides valuable insight into various module characteristics, including IV, s-parameters, power and harmonics and serves as essential part of the final product design. As a result, 34/31dBm output with 45/36% PAE in GSM/DCS bands was achieved for the entire TX module.

ACKNOWLEDGMENTS

The authors wish to thank many people at Skyworks who contributed to this work including: I. Khayo, I. Lalicevic, D. Evans, R. Burton, C. Jacobs, K. Frey, D. Britton, K. Crompton, D. Hirani, B. Bousquet, D. Bartle, R. Ramathan, W.-J. Ho, P. Zampardi, and M. Glasbrener.

REFERENCES

- [1] R. Jos, "Technology developments driving evolution of cellular phone power amplifiers to integrated RF front-end modules," IEEE Journal of Solid-State Circuits, No. 9, Vol. 36, Sep. 2001, pp. 1382-1389.
- [2] D. Wu, M. Frank, N. Hendin, and S. Yajima, "Radio front-end module technologies and design for multi-band/mode cellular handsets," IMS-2003 short course digest on "RF FEM's for cellular phone and WLAN applications," 2003.
- [3] P. DiCarlo, S. Boerman, R. Burton, H.- C. Chung, D. Evans, M. Gerard, J. Gering, I. Khayo, L. Lagrandier, I. Lalicevic, P. Reginella, S. Sprinkle, and Y. Tkachenko, "A highly integrated quad-band GSM TX-front-end-module," Proceedings of the 25th GaAs IC Symposium, Nov. 2003, pp. 280-283.
- [4] C.-J. Wei, J. Gering, S. Sprinkle, A. Klimahsow, and Y. A. Tkachenko, "Modified VBIC-model for InGaP/GaAs HBTs," Digest of 2002 APMC, Kyoto, Japan, WEOF10, Nov. 2002
- [5] C. Wei, D. Johnson, O. Manzura, Y. Tkachenko and D. Bartle, "Large-signal model of triple-gate MESFET/PHEMT for switch applications," in 1999 Internat. Microwave Symp. Dig. pp. 745-749
- [6] C. J. Wei, Y. A. Tkachenko, and D. Bartle, "A new analytic model for power E-mode PHEMTs and its optimum power operation," IEEE Transactions on Microwave Theory and Techniques, Vol. MTT-50, Jan.2002, pp.57-61